Nuclear Magnetic Resonance Studies of Multi-site Chemical Exchange. II. Hindered Rotation in *N*,*N*-Dimethyl Carbamyl Fluoride

L. W. REEVES AND K. N. SHAW
Department of Chemistry, University of Waterloo, Waterloo, Ontario

Received March 1, 1971

The matrix formulation of the Bloch equations including chemical exchange reported earlier is extended to include indirect spin–spin coupling in first-order spectra. The ABX ($J_{AB} = 0$) spin system is treated in detail and particular attention is paid to the determining effect on the nuclear magnetic resonance (n.m.r.) lineshapes of the relative signs of the coupling constants J_{AX} and J_{BX}. The hindered rotation for *N*,*N*-dimethyl carbamyl fluoride in CCl_4 as solvent has been studied using a complete ^1H n.m.r. lineshape analysis and the activation parameters obtained are: $\Delta G^{\neq} = 18.1 \pm 0.6$ kcal mol^{-1}, $\Delta H^{\neq} = 17.7 \pm 0.6$ kcal mol^{-1}, and $\Delta S^{\neq} = -1.4 \pm 2.1$ cal deg^{-1} mol^{-1} at 25 °C.

The complete lineshape fits give very precise values of the relative shifts (16.5 mol% in CCl_4) of the methyl groups and of the coupling constants J_{AX} (0.30 ± 0.05 Hz) and J_{BX} (0.80 ± 0.05 Hz) at all temperatures. A 40% change in J_{BX} (1.10 ± 0.05 Hz) is observed in neat DMCF from a lineshape fit at −15 °C. The origin of changes in chemical shifts with temperature and J_{BX} with solvent is discussed.

La forme matricielle des équations de Bloch appliquée à l'échange chimique et rapportée précédemment est développée pour tenir compte des couplages spin–spin indirects dans les spectres au premier ordre. Le système de spin ABX (avec $J_{AB} = 0$) est traité en détail, en portant une attention particulière à l'effet déterminant des signes relatifs des constantes de couplage J_{AX} et J_{BX} sur la forme des raies du spectre r.m.n.

L'étude de la rotation restreinte du fluorure de *N*,*N*-diméthyle carbamyle en solution dans CCl_4 par une analyse complète de forme de raies r.m.n. du proton a donné les paramètres d'activation: $\Delta G^{\neq} = 18.1 \pm 0.6$ kcal mol^{-1}, $\Delta H^{\neq} = 17.7 \pm 0.6$ kcal mol^{-1} et $\Delta S^{\neq} = -1.4 \pm 2.1$ cal deg^{-1} à 25 °C.

Le calcul complet des formes de raies donne des valeurs très précises pour les déplacements relatifs (16.5 mol% dans CCl_4) des groupes méthyles et les constantes de couplage J_{AX} (0.30 ± 0.05 Hz) et J_{BX} (0.80 ± 0.05 Hz) à toutes les températures. Une variation de 40% de J_{BX} (1.10 ± 0.05 Hz) est observée dans le DMCF pur d'après un calcul de forme de raies à −15 °C. L'origine des variations de déplacement chimique avec la température et de J_{BX} avec le solvant est discutée.

Canadian Journal of Chemistry, 49, 3671 (1971)

Introduction

The Bloch equations (1) have been modified to include chemical exchange effects (2–4), in first-order spectra, and have allowed a simple phenomenological description of n.m.r. lineshape characteristics. In the first paper in this series (5), a concise matrix formulation of the modified Bloch equations has been presented as a basis for a series of experimental studies of a wide range of chemical systems. This formulation accommodates a general first-order *n*-site exchange system and a complete description of all rate processes is contained in a single $n \times n$ matrix. Such a theoretical approach allows an efficient routine analysis for rate constants and activation parameters.

The effect of chemical exchange on spin–spin multiplets in first-order n.m.r. spectra was recognized in the original work of Gutowsky *et al.* (2, 6), and various approximate analytical expressions have been developed to derive kinetic data for specific cases (7–10). Only recently, however, have complete lineshape analyses been applied to multi-site exchange systems with *J*-coupling (11–15). Inconsistent analyses are still appearing in the literature, however, and very little reliable kinetic data is available. Thus this paper outlines the inclusion of *J*-coupling for the representative ABX ($J_{AB} = 0$) spin system. It is shown that, from a complete lineshape analysis in the first-order limit, the detailed form of chemical exchange and additional relaxation processes and also the relative signs of indirect spin–spin coupling constants may be readily determined. The experimental case chosen, namely the hindered rotation in *N*,*N*-dimethyl carbamyl fluoride (DMCF), is particularly problematical because of a very small chemical shift between two environmental sites and relatively small J_{AX} and J_{BX} values.

A unified theory of exchange modified n.m.r. lineshapes has been presented by Binsch (16). This theory using the Liouville operator formalism is inclusive of the cases discussed in this paper, but a detailed description of the lineshapes for first-order spectra (of the form observed for *N*,*N*-dimethyl amides) is included here to allow a lucid illustration of the inclusion of *J*-coupling and, in particular, to emphasize the effects of the relative signs of the coupling constants as discussed briefly in an earlier paper (12). The matrix formulation presented here follows directly from the stochastic exchange model discussed in the first paper in this series (5) and all the equations used are also applicable to second-order (tightly coupled) spin systems. That is, the diagonal matrix $\boldsymbol{\Omega}$, *cf.* eq. 19 in ref. 5, defining the Larmor frequencies for spin-sites in the first-order limit is replaced by an off-diagonal matrix with elements formally derived in terms of a superoperator (17–19) in a simple product function basis; and the intensity and population vectors $\boldsymbol{I}$ and $\boldsymbol{P}$, respectively, *cf.* eq. 20 in ref. 5, have zero elements corresponding to combination transitions. This independently developed matrix formulation is particularly amenable to numerical lineshape calculations and has been used for efficient iterative lineshape fitting, similar to that described in this paper, and will be discussed for specific examples of multi-site chemical exchange involving second-order spin systems in future publications.

Hindered rotation about the N—C bond in amides has been the subject of numerous n.m.r studies (20); but to date, reliable data for closely related chemical systems are very limited. Thus *N*,*N*-dimethyl carbamyl fluoride has been studied as a member of a series of halo-substituted amides to allow a correlation of the barriers to rotation with bonding parameters from molecular orbital calculations. Also, although this compound is well known as a specific enzyme inhibitor (21, 22), no information is available on its electronic structure as compared with other amides of importance in biological systems (23). The parent compound carbamyl fluoride is stable only at a low temperature (24) and hence the barrier to rotation cannot be measured for this particular amide, as is the case for other carbamyl halides and carbamyl pseudo-halides. The electronic interactions of interest, namely those between the carbonyl and amide groups and a given C-substituent X in the general structures 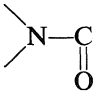 $\mathrm{>N{-}\underset{\underset{\displaystyle O}{\|}}{C}{-}X}$, have very similar comparative characteristics for the parent amides and a corresponding *N*,*N*-dimethyl amide series. As the latter amides are readily accessible, this particular series has been chosen for a quantitative comparison of bonding characteristics in C-substituted amides.

Chemical Exchange Spin-sites, ABX Spin System

A normal multi-site n.m.r. exchange system, in the first-order limit, is considered in terms of distinct sites (2, 5) of differing Larmor frequency, ω_i, such that each site may be associated with a specific molecular electronic environment and corresponding relative chemical shift, Ω_i. This concept of exchange sites may now be extended to spin systems including *J*-coupling. As the simple first-order ABX ($J_{AB} = 0$) spin system includes all the features of a general analysis, and is applicable to a study of hindered rotation in *N*,*N*-dimethyl carbamyl fluoride, this particular system will be considered in detail. The spin Hamiltonian for this system may be expressed in the form

$$[1] \quad \begin{aligned} H &= H_0 + H_\Omega + H_J^{(1)} \\ &= -\omega_0[I_{zA} + I_{zB} + I_{zX}] + \Omega[I_{zA} - I_{zB}] \\ &\quad + \Omega_X I_{zX} + J_{AX} I_{zA} I_{zX} + J_{BX} I_{zB} I_{zX} \end{aligned}$$

H_0 is a generalized Zeeman term and ω_0 is a reference Larmor frequency (rad s^{-1}). An independent frequency variable x may now be defined as $x = \omega - \omega_0$ (5), where ω is the frequency of the irradiating r.f. magnetic field. H_Ω is the chemical shift term in which $\Omega_A = -\Omega$ and $\Omega_B = \Omega$ with $\omega_0 = (1/2)\,(\omega_A - \omega_B)$ and $\Omega_A = \omega_A - \omega_0$. $H_J^{(1)}$ is the *J*-coupling term as $H_J^{(2)} = (1/2)\{J_{AX}[I_A^+ I_X^- + I_A^- I_X^+] + J_{BX}[I_B^+ I_X^- + I_B^- I_X^+]\}$ may be neglected in a first-order ($J_{ij} \ll |\Omega_i - \Omega_j|$) determination of spectral transition frequencies and intensities (25). The $H_J^{(2)}$ term, however, has been shown to give rise to a spin–spin relaxation mechanism which may be described by Bloch type equations for a weakly coupled spin system (26). The effect of such a relaxation in addition to chemical exchange is not included in the present work. In the usual I_Z-representation with simple product basis functions, ϕ_l, the Hamiltonian given in eq. 1 is diagonal and hence all terms correspond to secular energies determining the transition frequencies listed in Table 1. As is well known, two relative sign combinations are possible for J_{AX} and J_{BX} (25) and thus it is initially assumed that $J_{AX} > 0$ and $J_{BX} > 0$. The AB-part of the ABX spectrum consists of the four transitions (each

TABLE 1
(*a*) Transition frequencies for ABX ($J_{AB} = 0$) spin system

Transition number*	Transition type	Energy levels†	Frequency x
1	A	(1,3), (2,4)	$-\Omega-\frac{1}{2}J_{AX}$
2	A	(5,7), (6,8)	$-\Omega+\frac{1}{2}J_{AX}$
3	B	(1,2), (3,4)	$\Omega-\frac{1}{2}J_{BX}$
4	B	(5,6), (7,8)	$\Omega+\frac{1}{2}J_{BX}$
1	X	(1,5)	$-\Omega_X-J_+$‡
2	X	(3,7)	$-\Omega_X-J_-$
3	X	(2,6)	$-\Omega_X+J_-$
4	X	(4,8)	$-\Omega_X+J_+$

*These transition numbers correspond to those used in Figs. 1 and 3.
†The bracket (l,m) refers to energy levels E_l and E_m, and corresponding eigen-functions ϕ_l and ϕ_m.
‡ $J_\pm = (1/2)(J_{BX} \pm J_{AX}); J_{BX} > J_{AX} > 0$.

(*b*) Basis (eigen) functions (ϕ_l) for ABX spin system, $I = 1/2$ nuclei

l	ϕ_l	l	ϕ_l
1	$\alpha\alpha\alpha$	5	$\alpha\alpha\beta$
2	$\alpha\beta\alpha$	6	$\alpha\beta\beta$
3	$\beta\alpha\alpha$	7	$\beta\alpha\beta$
4	$\beta\beta\alpha$	8	$\beta\beta\beta$

of which is doubly degenerate for $J_{AB} = 0$) shown in Fig. 1(*a*), where the J-couplings with the X-spin determine effective Larmor frequencies $x = -\Omega \pm (1/2)J_{AX}$ and $x = \Omega \pm (1/2)J_{BX}$. These frequencies may be associated with four distinct exchange sites, analogous to the two environmental sites with Larmor frequencies $x = \pm\Omega$. Thus in general, in the presence of exchange, a basic environmental (chemical shift) site with an associated X-spin state may be referred to as *spin site-j*, with Larmor frequency x_j. In this manner, for the couplings as given above, spin site-1 corresponds to a basic A-site associated with an α X-spin state as shown by the eigenfunctions corresponding to the energy levels determining the transition frequency $x_1 = -\Omega - (1/2)J_{AX}$: ($\alpha\alpha\alpha$, $\beta\alpha\alpha$) and ($\alpha\beta\alpha$, $\beta\beta\alpha$). For a molecular system not having a preferred conformation (equal population exchange system) all transition intensities in the AB-part of the spectrum are equal, as are those in the X-part, in the absence of exchange. The X-part of the ABX spectrum consists of the four transitions shown in Fig. 3(*a*).

In terms of a stochastic theory (3, 27) for exchange effects in a first-order spin system, the nuclear magnetization associated with spin site-j may be considered in terms of a spin isochromat (28) $M(x_j,\phi_j)$ with Larmor frequency x_j and phase ϕ_j (27) and a magnitude proportional to the fractional population P_j (5). In the absence of exchange, these spin isochromats precess independently about the direction of the static applied magnetic field and a transverse relaxation time T_{2j} describes the coherent isochromat dephasing (28), and Lorentzian distribution of Larmor frequencies about x_j, associated with local magnetic field inhomogeneity. In the presence of chemical exchange, characterized by a rate constant k, individual spin isochromats are involved in a random transfer between spin-sites. Conversely, it may be considered that each spin isochromat experiences a randomly fluctuating local magnetic field with a fundamental frequency component k rad s^{-1}. Thus an exchange process gives rise to an incoherent isochromat dephasing and a modulation of the Larmor frequencies x_j. The assumptions inherent in a stochastic description of exchange effects may now be summarized as follows:

(*i*) the isochromat $M(x_j,\phi_j)$ remains in spin

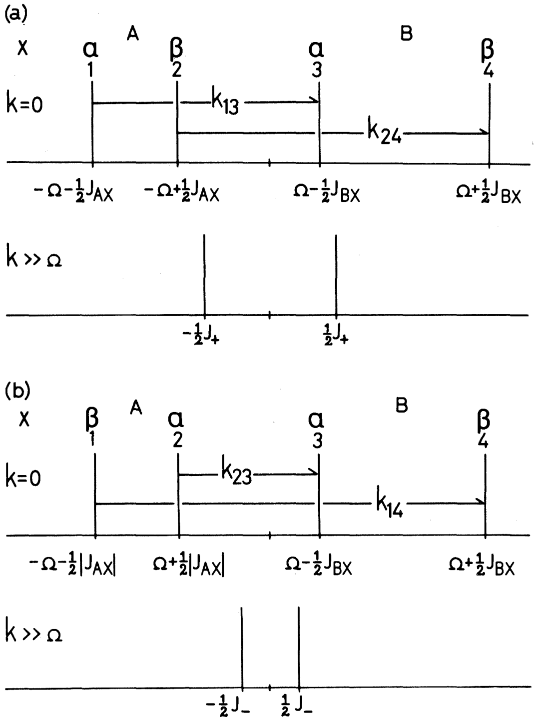

FIG. 1. AB-part of first-order ABX ($J_{AB} = 0$) spectrum in the limits of no exchange and fast exchange ($k \gg \Omega$): (*a*) $J_{BX} > J_{AX} > 0$ and $J_+ = (1/2)(J_{BX} + J_{AX})$; (*b*) $J_{BX} > 0$, $J_{AX} < 0$ with $J_{BX} > |J_{AX}|$ and $J_- = (1/2)(J_{BX} - |J_{AX}|)$. The basic A and B environmental sites are indicated along with the X-spin state corresponding to each AB-exchange spin-site.

site-*j* with a mean lifetime τ_j until a random instantaneous transfer to a different site takes place due to a chemical exchange process, such that precessional effects in the transfer interval may be neglected;

(*ii*) the site lifetime τ_j is independent of the associated spin–spin and spin–lattice relaxation times, T_{2j} and T_{1j}, respectively;

(*iii*) individual spin isochromats relax independently except for site transfer effects; and

(*iv*) for $M(x_j,\phi_j)$ in spin site-*j* there is a constant probability per unit time, k_{ji}, for transfer *from site-j into site-i*, this probability being inversely proportional to the fractional site population P_j.

Under these assumptions, the spin-site lifetime τ_j and associated rate constants are related by

$$[2] \qquad \sum_i k_{ji} = \tau_j^{-1}$$

where i ($i \neq j$) includes all allowed transfer sites connected with site-*j*, and $\tau_j > T_{1j}$. Also, in accordance with the principle of detailed balance for rate processes, spin-site populations and rate constants for any two sites satisfy the condition

$$[3] \qquad P_i k_{ij} = P_j k_{ji}$$

In terms of this stochastic model, an intramolecular mutual exchange in an ABX spin system (for example, hindered internal rotation) is described by a single first-order rate constant and will be assumed to give a transfer of nuclear magnetization between *spin-sites* distinguished by the chemical shifts for A- and B-spins, $-\Omega$ and $+\Omega$, respectively. All possible transfers between the four AB spin-sites may be represented by

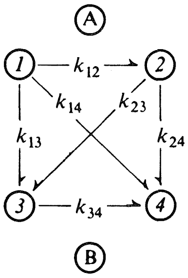

In accordance with assumption (*i*) above, it must be assumed that the X-spin state is *unchanged* during an AB spin-site transfer and hence the allowed transfers are *1* ↔ *3* and *2* ↔ *4* as readily seen by comparison of the eigen-functions associated with the transitions *1*, *3* and *2*, *4* in Table 1. That is, transitions *1* and *3* are A- and B-spin transitions, respectively, where all eigen-functions involved have an α X-spin part as shown in Fig. 1(*a*). For a mutual intramolecular exchange, this stochastic model is consistent with a quantum-mechanical treatment (29, 30) in that it may be considered that the molecular system following a nuclear spin-site transfer has a spin Hamiltonian differing only in interchanged magnetic properties for the A- and B-spins. An exchange operator E defined by $E|\alpha\alpha\xi_X\rangle = |\alpha\alpha\xi_X\rangle$ and $E|\alpha\beta\xi_X\rangle = |\beta\alpha\xi_X\rangle$, where ξ_X is the X-spin part of the product basis function, then determines exactly those transitions involved in AB spin-site transfers as allowed above. In an intramolecular exchange, the nuclear spin states for an individual molecule following a spin-site transfer are determined completely by the original states. This is actually the fundamental difference between such a process and an intermolecular exchange in which the overall state of an individual molecule following spin transfer depends upon the original state of this molecule and also the state of the interacting molecule. Therefore, if the X-spin undergoes an intermolecular exchange all AB spin-site transfers as depicted above are allowed as the X-spin state may now be *changed* in this exchange process. For example, spin-sites *1* and *2* differ only in the X-spin state as shown in Fig. 1(*a*). Such a spin-site transfer may also be considered to correspond to a spin–lattice relaxation mechanism for the X-spin; and in particular, the correlation time τ_C for a quadrupolar relaxation process may be comparable to the AB spin-site lifetime τ_j. Such a mechanism also leads to the effective transfers *1* ↔ *4*, *2* ↔ *3*, and *3* ↔ *4*. The effect of this additional relaxation process will depend upon the parameters $(\tau_C J_{AX})^{-1}$ and $(\tau_C J_{BX})^{-1}$, and hence in many first-order spin systems in the liquid phase such an effect may be described by a pseudo-secular contribution to the transverse relaxation time T_{2j}.

General lineshape characteristics for chemical exchange in the AB-part of a first-order ABX spectrum are concisely described through a 4 × 4 rate matrix, $\mathbf{K}$, as defined in the first paper of this series (5). In the zero saturation limit, a complex lineshape function $G(x)$ may then be expressed in the form

$$[4] \qquad G(x) = A\,\boldsymbol{I}.\mathbf{S}.[\boldsymbol{\Lambda} + (1/T_2 + \mathrm{i}x)\mathbf{I}]^{-1}.\mathbf{S}^{-1}.\boldsymbol{P}$$

in which $\mathbf{\Lambda}$ is the diagonal matrix corresponding to a matrix $[\mathbf{K} - \mathrm{i}\mathbf{\Omega}]$, the diagonal matrix $\mathbf{\Omega}$ being defined by the spin-site Larmor frequencies, x_j, in terms of the independent frequency variable x. $\mathbf{S}$ is the matrix which diagonalizes $[\mathbf{K} - \mathrm{i}\mathbf{\Omega}]$, *viz.*, $\mathbf{\Lambda} = \mathbf{S}^{-1}.[\mathbf{K} - \mathrm{i}\mathbf{\Omega}].\mathbf{S}$. $\boldsymbol{P}$ is the spin-site fractional population column vector and $\boldsymbol{I}$ is a transition intensity row vector. It has been implicitly assumed that T_{2j} is the same for all spin-sites in defining the relaxation matrix $\mathbf{T}_2$ as the scalar matrix $(1/T_2)\mathbf{I}$, where $\mathbf{I}$ is the 4×4 unit matrix. This simplification is usually valid in that non-secular relaxation processes (26, 29), as described by off-diagonal elements in $\mathbf{T}_2$, are negligible. However, it is to be noted that the relaxation processes associated with the J-coupled X-spin, and considered in terms of effective spin-site transfers above, are equivalently described by such off-diagonal elements. In this manner, quadrupolar relaxation effects are very simply incorporated in to eq. 4.

The matrix $\mathbf{K}$ describing intramolecular exchange effects in the AB-part of the equal population ABX ($J_{AB} = 0$) spin system with $J_{BX} > J_{AX} > 0$, and spin-sites as ordered in Fig. 1(*a*), is given (5) in terms of the rate constant k s^{-1} as

$$\mathbf{K} = \begin{pmatrix} k & 0 & -k & 0 \\ 0 & k & 0 & -k \\ -k & 0 & k & 0 \\ 0 & -k & 0 & k \end{pmatrix}$$

In accordance with eq. 2, the diagonal element K_{jj} is equal to the inverse spin-site lifetime τ_j^{-1}. The elements of the diagonal $\mathbf{\Omega}$ matrix are simply the transition frequencies listed in Table 1, and the vectors $\boldsymbol{P}$ and $\boldsymbol{I}$ have equal elements 0.25 and 1.0, respectively. Equation 4 now allows a very efficient computation of the steady-state n.m.r. absorption mode lineshape function, $V(x)$, as the real part of $G(x)$. Lineshapes have been calculated for the AB-part of the ABX spectrum defined by: $\Omega = 4.0$ Hz, $J_{AB} = 0$, $J_{AX} = 2.0$ Hz, $J_{BX} = 5.0$ Hz, and $T_2 = 0.64$ s (0.5 Hz full width at half-maximum), and are shown in Fig. 2(*a*) for rate constants in the range $0 \leqslant k \leqslant 200\ \mathrm{s}^{-1}$. These lineshapes are normalized independently of k, through the constant A in eq. 4, and the spectrum limits are ± 20 Hz. In the limit of fast exchange ($k \gg \Omega$) the spectrum reduces to a doublet. This feature is characteristic of an A_2X spin system and is consistent with the expectation that in this limit basic A- and B-sites become equivalent. As shown in Fig. 1(*a*), for J_{AX} and J_{BX} of the *same sign* the doublet splitting is J_+, where $J_+ = (1/2)(J_{BX} + J_{AX})$.

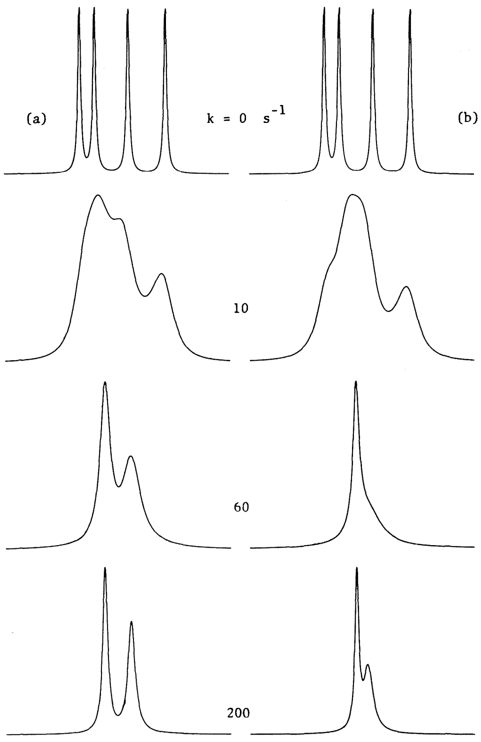

FIG. 2. Intramolecular exchange lineshape function, $V(x)$, for the AB-part of first-order ABX ($J_{AB} = 0$) spectrum; (*a*) $J_{BX} > J_{AX} > 0$; (*b*) $J_{BX} > 0$, $J_{AX} < 0$ and $J_{BX} > |J_{AX}|$.

Now for a spin system with J_{AX} and J_{BX} of *different sign*, the spin–spin coupling term in the Hamiltonian given in eq. 1 may be expressed as $-|J_{AX}|I_{zA}I_{zX} + J_{BX}I_{zB}I_{zX}$, where it is assumed that $J_{AX} < 0$ and $J_{BX} > 0$. The allowed transition frequencies are defined by substituting $-|J_{AX}|$ for J_{AX} in Table 1; and the AB-part of the spectrum for this spin system is shown in Fig. 1(*b*), in which the ordered transitions *1* and *2* now correspond to β and α X-spin states, respectively. In this case, the matrix $\mathbf{K}$ is

$$\mathbf{K} = \begin{pmatrix} k & 0 & 0 & -k \\ 0 & k & -k & 0 \\ 0 & -k & k & 0 \\ -k & 0 & 0 & k \end{pmatrix}$$

and this matrix determines the lineshapes shown in Fig. 2(*b*) for the parameters previously given. In the region of coalescence ($k \sim \Omega$) and in the fast exchange limit, for a given rate constant k, these lineshapes are distinctly different from those for J_{AX} and J_{BX} of the same sign, *cf.* Fig. 2(*a*). Therefore, in general, the *relative signs* of J_{AX} and J_{BX} may be determined directly by lineshape fitting of an exchange modified ABX spectrum. To date, this feature has apparently only been recognized in a few instances (12, 31). Of course, a further consequence of J_{AX} and J_{BX} having different signs is that the doublet splitting in the fast exchange limit is J_-, where $J_- = (1/2)(J_{BX} - |J_{AX}|)$ for $J_{BX} > |J_{AX}|$, as shown in Fig. 1(*b*).

The corresponding rate matrices, **K**, for a more general unequal population exchange system have elements determined by the relationship given in eq. 3. Thus for $J_{BX} > J_{AX} > 0$ it follows that $K_{31} = -k$ and $K_{13} = -(P_A/P_B)k$, where k is the first-order rate constant for transfer from spin-site *1* and P_A is the sum of fractional populations for the spin-sites associated with the A-type basic environmental exchange site. In this manner the doublet in the fast exchange limit is centered at $x = (1 - 2P_A)\Omega$ and it has a splitting given by $(1 - 2P_A)J_- + J_+$, which is equivalent to the weighted average coupling $P_AJ_{AX} + P_BJ_{BX}$. For $J_{BX} > 0$ and $J_{AX} < 0$, this doublet is centered as above but the splitting is now given by $(1 - 2P_A)J_+ + J_-$, where J_+ and J_- are as previously defined.

Exchange effects in the X-part of the ABX ($J_{AB} = 0$) spectrum under consideration are also described by 4 × 4 matrices **K** and **Ω** analogous to those already discussed. The X-part spectra in the absence of exchange and in the fast exchange limit ($k \gg J_{\mp}$) are represented as shown in Fig. 3. The corresponding absorption mode lineshapes (for the particular set of parameters previously defined) are shown in Fig. 4, and again the relative signs of J_{AX} and J_{BX} give rise to marked differences in the computed lineshapes. An example in the literature closely related to the ABX spin system is ^{15}N-formamide analyzed as an ABXY ($J_{AB} \neq 0$) system (32). Inspection of the X-part of the experimental spectrum at 75 °C clearly shows that J_{AX} and J_{BX} have the same sign, as now verified by double resonance methods (33, 34).

With respect to experimental n.m.r. lineshape fitting, an analysis of *both* the AB- and X-parts of an ABX spectrum allows a check on the internal consistency of the fitting procedure used to obtain rate constants for a given exchange process. Also, in general, lineshape fitting is most reliable in the region of coalescence. Now the coalescence condition for the AB-part of the spectrum is determined by the chemical shift difference 2Ω, whereas the same condition for the X-part is determined by the parameter $J_- = (1/2)(J_{BX} - J_{AX})$ (or $J_+ = (1/2)(J_{BX} + |J_{AX}|)$); and hence, if J_- (or J_+) and 2Ω differ significantly, a dual analysis may allow an accurate measurement of the specific rate constant k over an extended temperature range, which is critical in the determination of reliable activation parameters from the usual Arrhenius plot.

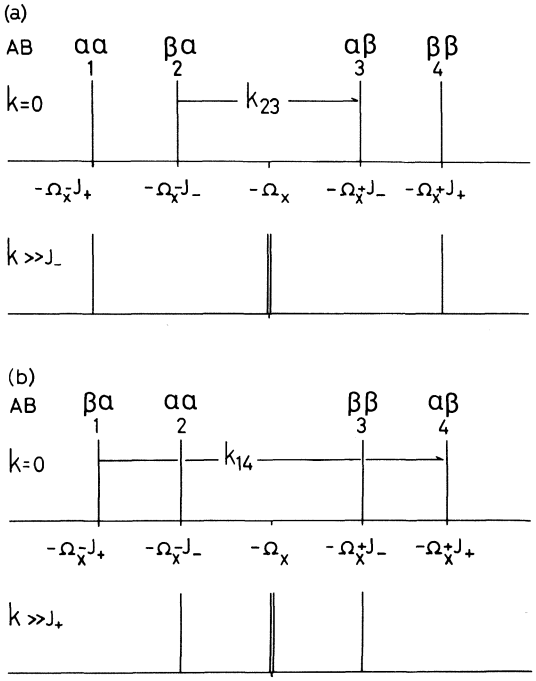

FIG. 3. X-part of first-order ABX ($J_{AB} = 0$) spectrum in the limits of no exchange and fast exchange ($k \gg J_{\mp}$): (*a*) $J_{BX} > J_{AX} > 0$ and $J_{\pm} = (1/2)(J_{BX} \pm J_{AX})$; (*b*) $J_{BX} > 0$, $J_{AX} < 0$ with $J_{BX} > |J_{AX}|$ and $J_{\pm} = (1/2)(J_{BX} \pm |J_{AX}|)$. The AB-spin states corresponding to each of the X-spin sites are shown for the ordered transitions.

Experimental

(A) Preparation of N,N-Dimethyl Carbamyl Fluoride (DMCF)

This compound was prepared by an exchange reaction between equimolar amounts of *N,N*-dimethyl carbamyl

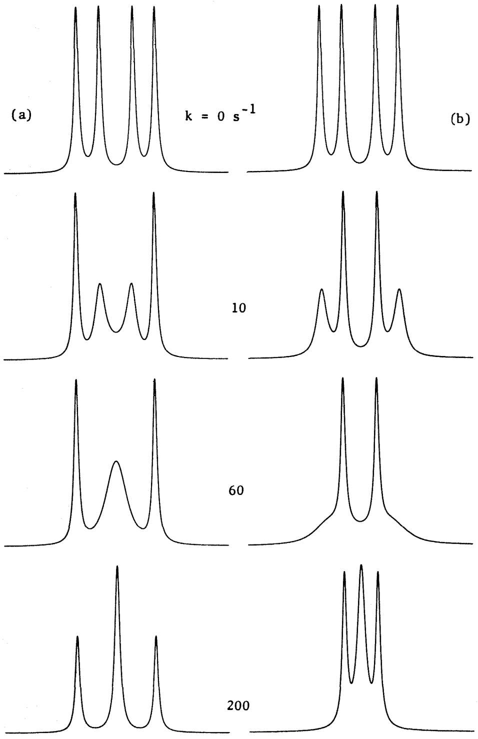

FIG. 4. Intramolecular exchange lineshape function, $V(x)$, for the X-part of an ABX ($J_{AX} = 0$) spectrum: (*a*) $J_{BX} > J_{AX} > 0$; (*b*) $J_{BX} > 0$, $J_{AX} < 0$, and $J_{BX} > |J_{AX}|$.

bromide (DMCB) and AgF, using acetonitrile as solvent, at room temperature. The yield was low ($\sim$15%), however, and hence use of SbF_3 as a fluorinating agent (35) allows a more efficient preparation. DMCB was obtained by saturating $\sim$10 g of *N,N*-dimethyl carbamyl chloride with HBr (36) at 0 °C. A N_2 stream was used to remove any HCl or Cl_2 formed and significantly increased the product yield. DMCF was purified by a spinning-band column distillation at 760 mm and 121 °C, the final product giving the elemental analysis: C 39.81 (39.58), H 6.58 (6.59) and F 20.68 (20.88), the values in parentheses being the calculated mole percentages for C_3H_6NOF.

(*B*) *Variable Temperature Nuclear Magnetic Resonance Spectra*

The ^1H n.m.r. spectra were obtained at 100 MHz with a Varian HA-100 spectrometer equipped with a V-6031 variable-temperature probe and temperature controller. The V-6031 controller maintains a preset temperature for the N_2 gas heating or cooling the sample, and the gas temperature is sensed at about 5 cm from the sample volume in the spectrometer receiver coil. Thus the sample temperature was measured before and after recording a spectrum using a standard methanol (or glycol) sample and interpolation of the —OH chemical shifts obtained in HA-mode using the data of Van Geet (37). The temperature thus determined is estimated to be accurate to ± 0.3 °C and was shown to be stable, within these limits, over a period of about 20 min. The spectra were recorded at sweep rates of 0.02 or 0.05 Hz s^{-1} to best approximate steady-state conditions, and with a low amplitude r.f. field ($\sim$0.02 mG) to minimize lineshape distortion due to saturation effects (5). At each temperature, to ensure reproducibility, at least four spectra were digitized and stored using a Fabritek FT-1074 computer interfaced with the HA-100. The interface unit, constructed in our laboratory, consists of a high input impedence differential amplifier for isolation of the A-D converter, logic circuitry for direct frequency calibration of the digital data and a digital/analog read-out for control of the HA-100 recorder. All frequencies were measured, using the V-4315 counter, with reference to TMS as an internal standard. An optimum H_0 field homogeneity was maintained over the temperature range -20 to 80 °C corresponding to a 0.4 Hz resolution ($T_2 = 0.8$ s) and a reference lineshape that best approximated a symmetrical Lorentzian shape. Dioxane ($\sim$2 mol%) was used to give an internal reference line, at a convenient frequency with respect to DMCF, and this linewidth was used to define the effective transverse relaxation time in the absence of chemical exchange, T_2, for DMCF. Wilmad PS-505 5 mm thin-walled sample tubes were used to attain reproducible spinning characteristics and field homogeneity control.

Lineshape measurements were made for DMCF as a 16.5 mol% solution in CCl_4. this solvent being chosen to minimize solvent–solute interactions (38). Solute–solute interactions are minimized in dilute solution. A dilution of DMCF is limited, however, by a decrease in the already small *N*-methyl chemical shift difference, 2Ω, for solute concentrations below the above value. The n.m.r. sample was degassed by the usual freeze–pump–thaw method, and sealed under N_2 at $\sim$1 atm to prevent refluxing at the elevated temperatures required.

(*C*) *Computation of Lineshapes*

The ^1H n.m.r. spectrum of DMCF corresponds to the A_3B_3 part of a first-order A_3B_3X ($J_{AB} = 0$) spectrum and hence may be analyzed as the AB-part of an ABX ($J_{AB} = 0$) system, as described in detail in the preceding section.

A Fortran-IV program designated GPLONK has been developed for the efficient iterative fitting of theoretical absorption mode multi-site exchange lineshapes to digital data. This program is based upon eq. 22*a* of ref. 5, which follows directly from the matrix formulation of the complex lineshape function, $G(x)$, *cf.* eq. 4 above. The input consists of (*i*) N experimental intensities (40–100) with arbitrary indexing, (*ii*) frequency calibration data, (*iii*) a baseline correction parameter, (*iv*) a specific normalization data point, (*v*) the linewidth of the internal reference line, and (*vi*) data defining the initial matrices K and Ω, and also the vectors $\boldsymbol{P}$ and $\boldsymbol{I}$, in eq. 4 above. The iterative fitting relies upon a rapidly convergent search using optimized parameter increments, where the rate matrix is varied following the general procedure outlined in ref. 5. An optional variation of spin-site frequencies is available, for the checking of temperature dependence. "Best fit" parameter values correspond to the usual sum of squares of deviations (39), while the lineshape fitting error is most conveniently considered as $\varepsilon = (1/N)\Sigma^{N}_{i=1}\,[V'(x_i) - V(x_i)]/V/x$, where $V'(x_i)$ and $V(x_i)$ are the normalized experimental and theoretical intensities, respectively, for the frequency x_i. For the 4 spin-site DMCF exchange system, the time for a complete fit and setting up of control arrays for a CALCOMP plotter on an IBM 360/75 system is less than 6 s, and this time is essentially independent of the number of data points involved as it is governed by the 4 × 4 matrix diagonalization and inversion in eq. 4 above.

(D) Calculation of Activation Parameters

The activation energy, E_a, for the hindered rotation in DMCF was determined from a least-squares fit to the usual Arrhenius equation

$$[5] \qquad \log k = -E_a/2.303\,RT + \log A$$

where k is the first-order rate constant describing the rotation at temperature T and A is the frequency factor for the rate process. A thermodynamical formulation of reaction rates (40) shows that the enthalpy and entropy of activation are given as

$$[6] \qquad \Delta H^{\ne} = E_a - RT$$

and

$$[7] \qquad \Delta S^{\ne} = R\,[2.303 \log (Ah/kT) - 1]$$

respectively, assuming E_a to be temperature independent. In eq. 7 h is Planck's constant and k is the Boltzmann constant. The free energy of activation, $\Delta G^{\ne}$, is then determined as $\Delta G^{\ne} = \Delta H^{\ne} - T\Delta S^{\ne}$ at 298 °K. The overall errors quoted for the activation parameters have been estimated from the statistical limits of 95% confidence for E_a and A (39) and a study of the systematic errors (41, 42) involved in the determination of the k values used in eq. 5.

Results and Discussion

In the A_3B_3 part of the A_3B_3X spectrum for DMCF the methyl group *trans* to the carbonyl oxygen, A_3, is assigned to low field of the B_3 group; as the former methyl group, in the planar molecular ground state, is within a shielding region associated with the magnetically anisotropic carbonyl group (43). A similar assignment for DMF (12) has been shown to be correct through use of the nuclear Overhauser effect (44); and also, the magnitude of the *trans* coupling constant, J_{BX} according to the above assignment, is shown to be greater than that of the *cis* coupling, J_{AX}, which is normal (33, 45) for substituted amides. The couplings determined for a dilute solution of DMCF in CCl_4 are $J_{AX} = 0.30 \pm 0.05$ Hz and $J_{BX} = 0.80 \pm 0.05$ Hz, the corresponding values for DMF being 0.35 and 0.06 Hz. Comparison with the related acetyl compounds CH_3CFO (J_{HF} = 7.6 Hz (42)) and CH_3CHO (J_{HH} = 2.9 Hz) shows the effects of the interposed N atom and the N—C partial double bond character, due to delocalization of the N lone pair electrons, in the amide systems. Assuming the hybridization (s-character) to be similar for π-bonding in DMCF and DMF, the relative magnitudes of J_{BX} and changes with respect to the acetyl systems may be considered to be directly related to the detailed form of the π-bonding in the 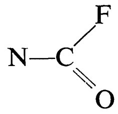 $\mathrm{N{-}C(F){=}O}$ and 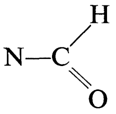 $\mathrm{N{-}C(H){=}O}$ groups.

Thus it is seen that the N–C double bond character is significantly greater for DMF, as $J_{BX}(\mathrm{DMF})/J_{HH} = 4.8$ and $J_{BX}(\mathrm{DMCF})/J_{HF} = 9.5$, and hence the barrier to hindered rotation about this bond is predicted to be higher in DMF. In fact, this is shown to be the case as the activation energy for hindered rotation in DMF is 20.8 ± 0.6 kcal mol^{-1} (12) and the activation energy for DMCF has now been determined as 18.3 ± 0.6 kcal mol^{-1}, *cf.* Table 3.

The couplings J_{AX} and J_{BX} in DMCF are temperature independent within ±0.05 Hz, as defined by the iterative lineshape fitting procedure; and for the 16.5 mol% CCl_4 solution, these couplings averaged to 0.55 ± 0.05 Hz at 78.2 °C in excellent agreement with the value expected for an A_6X spectrum in the fast exchange limit. Furthermore, the observed exchange modified lineshapes unambiguously lead to the conclusion that the signs of these couplings are the same. For example, in the region of coalescence at 44.9 °C the "best-fit" errors for the same and different signs were 1.2 and 2.0%, respectively, exemplifying the precision that may be attained through a total lineshape analysis. A typical experimental lineshape at this temperature is shown along with the corresponding "best-fit" theoretical lineshape in Fig. 5. At this point, it should be mentioned that the spin–spin couplings between methyl protons and the ^{14}N spin have been neglected in the lineshape analysis. Although a ^{1}H-$\{^{14}N\}$ double resonance study of N-substituted amides indicated that these couplings were negligibly small, the data available from further studies using ^{15}N-amides (34) leads to the ^{14}N coupling constants J_{NA} and J_{NB} of 0.7 and 0.8 Hz, respectively. However, it may safely be assumed that the methyl protons are completely decoupled by the quadrupolar ^{14}N spin–lattice relaxation process (46, 47).

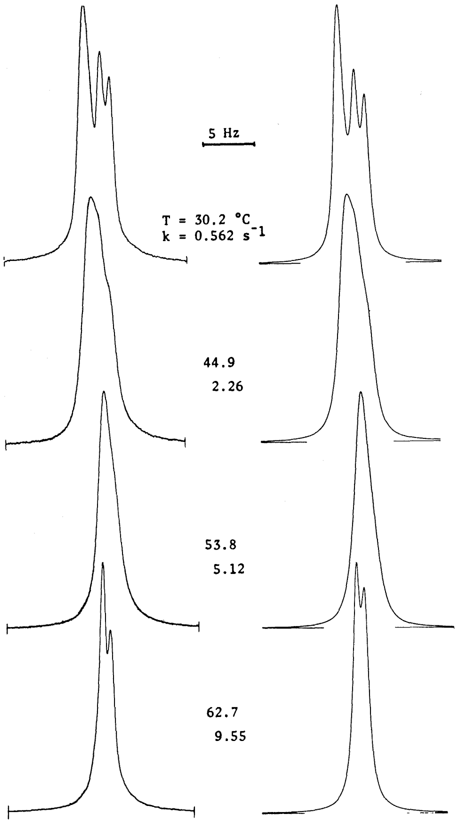

FIG. 5. Comparison of experimental and theoretical exchange lineshapes for DMCF.

In general, indirect spin–spin couplings are relatively insensitive to intermolecular interactions. In the case of a highly polar amide such as DMCF (μ = 4.02 D (48)) in a non-polar solvent, however, electrostatic solute–solute interactions may stabilize the polarized ground-state resonance form 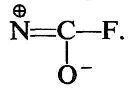 $\overset{\oplus}{N}{=}\underset{\underset{O^-}{|}}{C}{-}F$. An increased contribution from this structure then leads to an enhanced coupling between the ^{19}F spin and methyl protons due to the change in N—C double bond character. Such an effect has been observed in that J_{BX} = 1.10 ± 0.05 Hz for neat DMCF, as determined from a complete lineshape fit at −15 °C. This is an increase of about 40% over the same coupling for dilute CCl_4 solutions *cf.* Table 2, and thus it appears that the CCl_4 solvent breaks down a specific solute–solute interaction, probably leading to a simple dimeric form (11), between DMCF molecules. As this coupling constant is unchanged on further dilution, as shown in Table 2, it may be assumed that the dimer concentration is minimal for the 16.5% solution chosen for an accurate determination of kinetic parameters.

TABLE 2. ^1H n.m.r. data for DMCF, 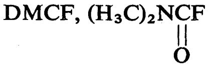 $(H_3C)_2N\underset{\underset{O}{\|}}{C}F$

(*a*) 16.5% solution in CCl_4

Temperature (°C)	ω_0 (Hz)*	2Ω (Hz)†
−15.2	−295.15±0.05‡	2.20±0.05‡
−5.5	−294.75	2.10
8.3	−294.40	2.00
15.6	−294.10	1.90
30.2	−293.55	1.75
44.9	−293.15	1.70
53.8	−292.80	1.60
62.7	−292.60	1.50
−78.2	−292.15	1.40

$J_{BX} = 0.80 \pm 0.05$, $J_{AX} = 0.30 \pm 0.05$ Hz‡

*$\omega_0 = (1/2)(\omega_A + \omega_B)$, determined with respect to TMS internal reference at 100 MHz and constant field.

†$2\Omega = \omega_B - \omega_A$, see text and ref. 5.

‡These error bounds are those used in the iterative lineshape fitting procedure.

(*b*) 7.5% solution in CCl_4

2Ω = 3.6 ± 0.1 Hz (220 MHz) at 22 °C
= 1.6 ± 0.1 (100 MHz) 24 °C
J_{BX} = 0.8, J_{AX} = 0.3 Hz

(*c*) Neat DMCF

2Ω = 1.2 ± 0.1 Hz (100 Hz) 30 °C
J_{BX} = 1.1, J_{AX} = 0.4 Hz

Chemical shifts are usually more sensitive to intermolecular interactions, and indeed the chemical shifts for the methyl groups in DMCF (and the shift difference 2Ω) are solvent-, concentration-, and temperature-dependent, as shown in Table 2 and Fig. 6. These chemical shifts are predominantly due to the combined effect of the magnetic susceptibility anisotropies associated with the C—F and C═O bonds. It may be considered that the NCO and NCF bond angles are both close to 120° for approximately regular sp^2 hybridization of the C atom,[1] and thus the small methyl chemical shift difference (~0.01 p.p.m.)

---

[1] The structure of DMCF has not been determined experimentally, but comparison of the structural data available for formamide (49), acetaldehyde (50), and acetyl fluoride (51) leads to ∠NCO = 128° and ∠NCF = 112.5°. These bond angles also correspond to a minimum energy configuration in the CNDO/2 s.c. approximation (52).

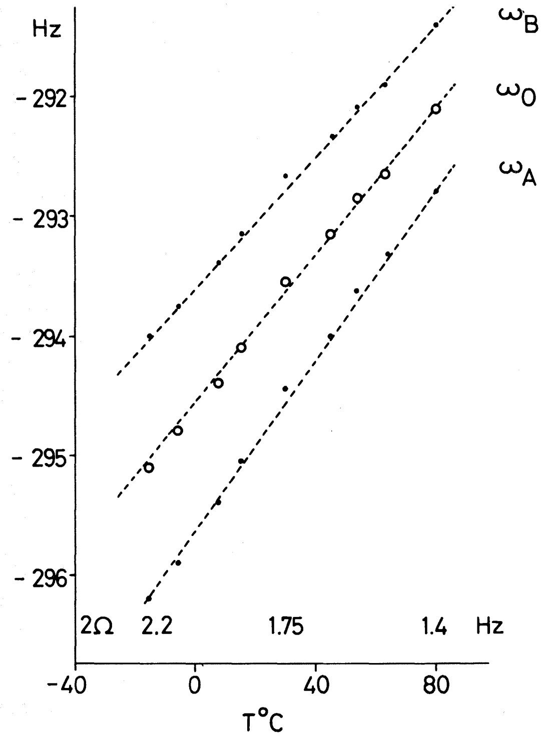

FIG. 6. Temperature dependence of *N*-methyl chemical shifts for DMCF, 16.5% in CCl_4, at 100 MHz.

implies that the charge distributions localized in these two bonds are of similar forms as the methyl groups *cis* and *trans* to the carbonyl group are in shielding regions having very nearly identical characteristics. This is to be compared with the shielding regions for the methyl groups in DMF, due to a carbonyl group only, giving $2\Omega = 17.5$ Hz at 100 MHz (~0.2 p.p.m.). As the C=O magnetic anisotropy is due to the axially asymmetric π-electron distribution in this group, it follows that delocalization of fluorine 2pπ-electrons, as represented by the resonance form 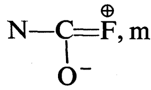 $\mathrm{N{-}\underset{O^-}{\underset{|}{C}}{=}\overset{\oplus}{F}}$, may be significant in the ground-state of DMCF. The small temperature dependence of 2Ω may be ascribed to an intermolecular dipolar association which affects the magnetic anisotropies of the C=O and/or C—F groups and which varies to a small extent with temperature. It should be noted that this temperature dependence, as determined from the complete lineshape analysis for DMCF in CCl_4, is only 0.008 p.p.m. over the temperature range −15.1 to 78.2 °C. All chemical shift variations, within ±0.05 Hz, were shown to be regular and reproducible over multiple lineshape fits, *cf.* Fig. 6.

The first-order rate constants, k s^{-1}, describing the hindered rotation about the N—C bond for DMCF as a 16.5 mol% solution in CCl_4 are listed in Table 3. These rate constants are average values obtained from multiple complete lineshape fits at each temperature. The corresponding temperature dependent chemical shifts are those given in Table 2, while the couplings J_{AX} and J_{BX} were assumed to be temperature independent. Because of the very small chemical shift difference 2Ω involved, the temperature interval for reliable k determinations is reduced to 66 °C and the overall k variation is only of the order of 200. The errors for the representative lineshape fits shown in Fig. 5 are maximal for very slow and very fast exchange[2] as accurately reproducible spectra for the DMCF four-site exchange system are very difficult to obtain in these limits, even with the stability afforded by a field-frequency locked spectrometer. For example, the average k value at 30.2 °C is 0.550 s^{-1} whereas six lineshape fits at this temperature gave values ranging

TABLE 3. Kinetic data for DMCF,

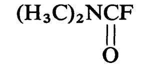
$\mathrm{(H_3C)_2N\underset{\underset{O}{\|}}{C}F}$

Temperature (°C)	k (s^{-1})	Error*
12.2	0.076	4.4
15.6	0.159	4.2
30.2	0.550	3.7
32.5	0.692	4.1
37.6	1.99	2.2
44.9	2.29	1.2
46.5	2.57	1.3
53.8	5.11	1.3
62.7	9.55	3.9
78.2	26.3	4.6

$E_a = 18.3 \pm 0.6$ kcal mol^{-1}
$\log_{10} A = 12.9$
$\Delta H^{\ddagger} = 17.7 \pm 0.6$ kcal mol^{-1}
$\Delta S^{\ddagger} = -1.4 \pm 2.1$ cal deg^{-1} mol^{-1}
$\Delta G^{\ddagger} = 18.1 \pm 0.6$ kcal mol^{-1}

*Percentage error for iterative lineshape fit, see text.

---

[2] These deviations may also arise from inherent inadequacies in the formulation of the lineshape function $V(x)$, such as the assumption of equal transverse relaxation times for all spin-sites in the absence of exchange. These relaxation times may be modified by time-dependent anisotropic chemical shift and anisotropic dipole–dipole interactions (54) and also by a cross-relaxation arising from these two interactions in DMCF.

from 0.362 to 0.944 s^{-1} with fitting errors of 3.5–6.2%. The resultant Arrhenius plot, however, is most satisfactory and is shown in Fig. 7. The activation parameters derived from the temperature independent Arrhenius constants, E_a and log A, and evaluated at 25 °C are given in Table 3.

For hindered rotations in amides the entropy of activation $\Delta S^{\ddagger}$ derived through complete n.m.r. lineshape analyses is normally relatively small; and in general, as increasing care is taken to remove systematic errors in obtaining kinetic data for a given rate process using n.m.r. methods the values of E_a and log A tend to increase (12, 41) leading to a value of $\Delta S^{\ddagger}$ close to zero. This entropy change is most probably due to a difference in the solvation structures, formed by dipolar solute–solvent association, for the ground and transition states of an amide. Such an association between the strongly polar DMCF and CCl_4 is possible, to some degree, through induced polarization of the solvent molecules. Therefore, if a solvation effect is dominant, a small increase in entropy is expected on formation of the transition state in amides as the dipole moment for this state is smaller than the moment for the ground state (52). For example, the calculated dipole moments, using s.c. theory, for the ground and transition states of carbamyl fluoride in minimum energy configurations are 3.98 and 3.41 D, respectively, which may be compared with the experimental value of 4.06 D (24). The entropy of activation determined here for DMCF, $\Delta S^{\ddagger} = -1.4 \pm 2.1$ cal deg^{-1} mol^{-1}, is formally negative but may only be considered to be very small. For the hindered rotation under consideration, a free energy change is expected to be determined primarily by intramolecular effects and hence this activation parameter is much simpler to interpret than the energy of activation which is sensitive to intermolecular effects. It is well known that there is a general tendency in rate processes in solution for enthalpy and entropy changes to compensate each other (53) so that the effective change in free energy is reduced and hence becomes less sensitive to external effects. The free energy of activation for DMCF has been determined as $\Delta G^{\ddagger} = 18.2 \pm 0.6$ kcal mol^{-1} and this particular parameter will be used in a forthcoming correlation of the bonding characteristics in a complete series of C-substituted *N*,*N*-dimethyl amides.

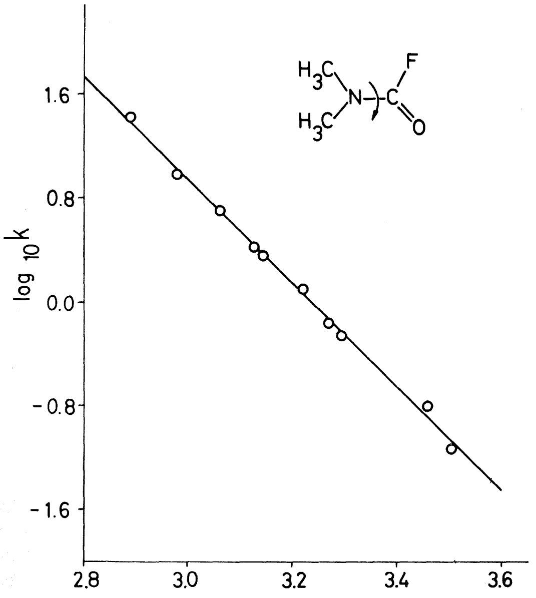

FIG. 7. Arrhenius plot for hindered rotation in DMCF, 16.5 mol% in CCl_4.

This work was supported by the National Research Council of Canada in grants to L.W.R. One of us (K.N.S.) gratefully acknowledges the financial support provided by a N.Z. Trust Lands Trust Overseas Scholarship and a British Columbia Sugar Refining Co. Scholarship while part of this work was undertaken at the University of British Columbia. We thank Mr. E. A. Allan for the preparation of DMCF.

1. F. BLOCH. Phys. Rev. **7**, 460 (1946).
2. H. S. GUTOWSKY, D. W. MCCALL, and C. P. SLICHTER. J. Chem. Phys. **21**, 279 (1953).
3. H. M. MCCONNELL. J. Chem. Phys. **28**, 430 (1958).
4. H. S. GUTOWSKY and C. H. HOLM. J. Chem. Phys. **25**, 1228 (1956).
5. L. W. REEVES and K. N. SHAW. Can. J. Chem. **48**, 3641 (1970).
6. H. S. GUTOWSKY and A. SAIKA. J. Chem. Phys. **21**, 1688 (1953).
7. E. GRUNWALD, A. LOEWENSTEIN, and S. MEIBOOM. J. Chem. Phys. **27**, 639 (1957).
8. A. LOEWENSTEIN and S. MEIBOOM. J. Chem. Phys. **27**, 1967 (1957).
9. M. TAKEDA and E. O. STEJSKAL. J. Am. Chem. Soc. **82**, 25 (1960).
10. M. T. ROGERS and J. C. WOODBURY. J. Chem. Phys. **66**, 549 (1962).
11. R. C. NEUMAN, D. N. ROARK, and V. JONAS. J. Am. Chem. Soc. **89**, 3142 (1967).
12. P. T. INGLEFIELD, E. KRAKOWER, L. W. REEVES, and R. STEWART. Mol. Phys. **15**, 65 (1968).
13. A. PINES and M. RABINOVITZ. Tetrahedron Lett. **31**, 3529 (1968). M. RABINOVITZ and A. PINES. J. Am. Chem. Soc. **91**, 1585 (1969).

14. K. I. Dahlqvist and S. Forsen. Acta Chem. Scand. **24**, 662 (1970).
15. C. J. Creswell and R. K. Harris. J. Mag. Res. **4**, 99 (1971).
16. G. Binsch. J. Am. Chem. Soc. **91**, 1304 (1969).
17. C. N. Banwell and H. Primas. Mol. Phys. **6**, 225 (1963). U. Fano. Rev. Mod. Phys. **29**, 74 (1957).
18. G. Binsch. Mol. Phys. **15**, 469 (1968).
19. S. M. Cohen. J. Chem. Phys. **52**, 234 (1970).
20. H. Kessler. Angew Chem. (Int. Ed.) **9**, 219 (1970).
21. I. B. Wilson. J. Biol. Chem. **235**, 2312 (1960); **236**, 2292 (1961).
22. H. P. Metzer. J. Biol. Chem. **238**, 3432 (1963).
23. H. A. Scheraga. Adv. Phys. Org. Chem. **6**, 193 (1968). Academic Press, N.Y.
24. J. S. Rigden and R. H. Jackson. J. Chem. Phys. **45**, 3646 (1966).
25. P. L. Corio. Chem. Rev. **60**, 363 (1960).
26. I. Solomon. Phys. Rev. **99**, 559 (1955).
27. M. Bloom, L. W. Reeves, and E. J. Wells. J. Chem. Phys. **42**, 1615 (1964).
28. E. L. Hahn. Phys. Rev. **80**, 589 (1950).
29. A. G. Redfield. I.B.M. J. Res. Dev. **1**, 19 (1957).
30. J. I. Kaplan. J. Chem. Phys. **29**, 462 (1958). S. Alexander. J. Chem. Phys. **37**, 967 (1962).
31. K. I. Dahlqvist and S. Forsen J. Phys. Chem. **69**, 4062 (1965).
32. L. M. Piette and W. G. Schneider. Can. J. Chem. **38**, 681 (1960).
33. A. J. R. Bourne and E. W. Randall. Mol. Phys. **8**, 567 (1964).
34. R. J. Chuck, D. G. Gillies, and E. W. Randall. Mol. Phys. **16**, 121 (1969).
35. G. Schrader. British Intelligence Obj. Subcommittee Final Report No. 714 B.I.O.S. London. 1945.
36. Z. Arnold. Coll. Czech. Chem. Comm. **24**, 760 (1959).
37. A. L. Van Geet. Anal. Chem. **40**, 2227 (1968).
38. A. D. Buckingham, R. Schaefer, and W. G. Schneider. J. Chem. Phys. **32**, 1227 (1960).
39. L. G. Parralt. Probability and experimental error. J. Wiley and Sons, N.Y. 1961. p. 126.
40. K. J. Laidler. Chemical kinetics. McGraw-Hill, N.Y. 1965. p. 67.
41. A. Allerhand, H. S. Gutowsky, J. Jonas, and R. A. Meinzer. J. Am. Chem. Soc. **44**, 3185 (1966).
42. T. Drakenburg, K. I. Dahlqvist, and S. Forsen. Acta Chem. Scand. **24**, 694 (1970).
43. D. L. Hooper and R. Kaiser. Can. J. Chem. **43**, 2363 (1965); J. W. ApSimon, P. V. Demarco, D. W. Mathieson, W. G. Craig, A. Karim, L. Saunders, and W. B. Whalley. Tetrahedron, **26**, 119 (1970).
44. F. A. L. Anet and A. J. R. Bourne. J. Am. Chem. Soc. **87**, 5250 (1965).
45. E. W. Randall and J. D. Baldeschweiler. J. Mol. Spectrosc. **8**, 365 (1962).
46. S. Brownstein and V. Bystrov. Can. J. Chem. **48**, 243 (1970).
47. J. A. Pople. Mol. Phys. **1**, 158 (1958).
48. E. Bock and D. Iwacha. Can. J. Chem. **46**, 523 (1968).
49. R. J. Kurland and E. Bright-Wilson, Jr. J. Chem. Phys. **27**, 585 (1957).
50. R. W. Kilb, C. C. Lin, and E. Bright-Wilson, Jr. J. Chem. Phys. **26**, 1695 (1957).
51. L. Pierce and L. C. Krishner. J. Chem. Phys. **31**, 875 (1959).
52. K. N. Shaw and L. W. Reeves. Unpublished results.
53. J. E. Leffler. J. Org. Chem. **20**, 1202 (1955).
54. A. Abragam. The principles of nuclear magnetism. Clarendon Press, Oxford. 1962. Chap. 8.